BSTR, 2022, Vol 10, No 2, 29-39
https://doi.org/10.54987/bstr.v10i2.779

HIBISCUS PUBLISHER

BIOREMEDIATION SCIENCE AND TECHNOLOGY RESEARCH

Website: http://journal.hibiscuspublisher.com/index.php/BSTR/index

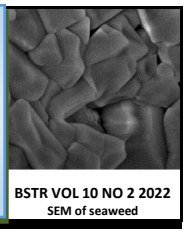

Response Surface Method for the Optimization of *E. cloacae* Strain UPM2021a Growth on Acrylamide as a Nitrogen Source

Aisami Abubakar[1], Motharasan Manogaran[2,3], Hafeez Muhammad Yakasai[4], Nur Adeela Yasid[2] and Mohd Yunus Shukor[2]*

[1]Department of Biochemistry, Faculty of Science, Gombe State University, P.M.B 127, Tudun Wada, Gombe, Gombe State, Nigeria.
[2]Department of Biochemistry, Faculty of Biotechnology and Biomolecular Sciences, Universiti Putra Malaysia, UPM 43400 Serdang, Selangor, Malaysia.
[3]Malaysia Genome and Vaccine Institute (MGVI) National Institute of Biotechnology Malaysia (NIBM) Jalan Bangi, 43000 Kajang, Selangor, Malaysia
[4]Department of Biochemistry, Faculty of Basic Medical Sciences, College of Health Science, Bayero University, Kano, PMB 3011, Nigeria.

*Corresponding author:
Mohd Yunus Shukor,
Department of Biochemistry,
Faculty of Biotechnology and Biomolecular Sciences,
Universiti Putra Malaysia,
UPM 43400 Serdang,
Selangor,
Malaysia.
Email: mohdyunus@upm.edu.my

HISTORY

Received: 19th Sep 2022
Received in revised form: 23rd Nov 2022
Accepted: 15th Dec 2022

KEYWORDS

Acrylamide
Acrylamide-degrading bacterium
E. cloacae
RSM
Box-Behnken

ABSTRACT

Acrylamide is often used in soil stabilization works. It is a neurotoxin and leachate from such stabilization works contaminate soils all around the world. *E. cloacae* strain UPM2021a which had been previously isolated and demonstrated the ability to degrade acrylamide was further studied for its critical parameters contributing to the optimum growth of acrylamide. The Box-Behnken design was utilized in optimizing the three previously identified significant components (pH, incubation time and acrylamide concentration). Of the three factors, acrylamide and pH were the significant factors. The response surface plot exhibited evidence of interactions. Predicted optimal conditions were determined using the "Numerical Optimisation" toolbox of the Design Expert software. Two optimal conditions were tested. The model predicted a maximum growth of 10.686 (95% C.I., 10.458 to 10.913) which was verified through experimental results with a growth of 11.257 (95% C.I., 11.051 to 11.462) with the actual results being near to the predicted values but was significantly higher than the predicted values. The second numerical optimization gave a solution with a predicted maximum growth of 9.305 log CFU/mL (95% C.I. from 9.011 to 9.614) which was verified through experimental results with a growth of 9.978 log CFU/mL (95% C.I. from 9.830 to 10.126) with the actual results were also significantly higher than the predicted values. This means that other methods which employ more runs such as CCD or a different optimization approach such as Artificial Neural Network may be employed in the future to close the difference between the model predicted and actual experimental values. Despite this, the RSM exercise gave far better growth on acrylamide than OFAT with a higher response of about 2 log CFU/mL unit indicating the utility of RSM over OFAT in the optimization of growth of this bacterium on acrylamide.

INTRODUCTION

Since 2005, commercial polyacrylamides are frequently contaminated by the poisonous monomer of acrylamide, a situation that has had a significant impact on our food supply chain. Agricultural land is polluted with acrylamides because of the 30% concentration of polyacrylamide in the Roundup herbicide. This issue, which needs to be addressed and remedied, can only be done so by the biological remediation of acrylamide [1]. Spencer and Schaumburg [2] found that acrylamide exposure caused cancer in laboratory animals, but it is unclear whether or not this is also the case in humans. During all stages of the spermatogenic process in mice, acrylamide was found to bind to DNA and mouse protamine, leading researchers to conclude that it is responsible for genetic damage [3]. Studies on the effects of acrylamide on rats have shown that it can cause a variety of

negative outcomes, including an increase in perinatal mortality, mutagenicity, clastogenicity, malignancies related to the endocrine system, and toxicity to male reproductive function [4]. Scientists have found that *Salmonella* TA100 and TA98 may be mutagenic when exposed to acrylamide (Yang et al., 2015).

The bone marrow of mice given an intraperitoneal injection of acrylamide at a dosage of 50 mg/kg showed an increase in chromosomal abnormalities after drug delivery. Lymphocytes from mice given acrylamide intraperitoneally at doses up to 125 mg/kg showed no significant increase in chromosomal abnormalities. This was observed when acrylamide was injected directly into the abdominal cavity [6].

Histological alterations in the seminiferous tubules caused by acrylamide also have an effect on the reproductive systems of male rats. The chemical is responsible for these histological changes. When inhaled or absorbed through the skin, acrylamide may create a burning sensation or rash. Something is amiss with the nervous system if you sweat excessively, feel lethargic, and/or have trembling in your tongue [2]. Due to its high-water solubility, acrylamide can be absorbed through the respiratory tract, the digestive system, the skin, and the placental barrier.

Acrylamides adduct levels in hemoglobin can be used as a proxy for the amount of acrylamide the general public is exposed to on the job. The research showed that 41 workers in an acrylamide production facility had problems with the biomarker haemoglobin adducts, which indicates neurotoxicity. An increase in haemoglobin adducts was found in workers at an acrylamide factory in China, suggesting that they were exposed to very high concentrations of the chemical [7]. Many cases of acute acrylamide poisoning have been reported in Japan as a result of acrylamide pollution in the country's water supply. There have been several reports of this happening to different persons.

A well that had been contaminated by a grouting operation at a depth of 2.5 meters was found to have an acrylamide content as high as 400 mg acrylamide/L, as discovered by Igisu et al. [8]. The results indicated that truncal ataxia and disorientation were among the symptoms experienced by the five participants who drank the contaminated water. These signs and symptoms are thought to be the result of acrylamide poisoning brought on by ingesting water. Since removing acrylamide using physicochemical methods is complicated and will be more expensive in some cases, such as in soil, the use of microorganisms for acrylamide remediation is gaining attention. Yeasts like *Rhodotorula* sp. [9], fungi like *Aspergillus oryzae* [10], and bacteria like *E. coli* [11-20] are among the microbes known to be able to use acrylamide as a source of energy.

Experiment planning in fundamental research is often done on an "intuitive" level. Biology experiments have traditionally been done "one factor at a time" (OFAT). In this technique, the output of the entity under study is examined while all other elements and variables are held constant. Though this approach may help researchers uncover important "major impacts," the interactions between its components will inevitably lead to suboptimum results. Due to the complexity of the process, a wide variety of inputs must be controlled for the best results. Although various studies on process optimization have used OFAT to improve responsiveness, optimizing more complex procedures would require an understanding of the linkages between components. For OFAT, one axis is optimized before moving on to the next.

The global maximum that maximizes the output variable may be determined if, by some stroke of luck, the research was started reasonably in the first place, although this is extremely unlikely [21-25]. A more rigorous strategy for analyzing experimental point placement and reaction, the response surface methodology (RSM). When there are few variables at play, a Taguchi or full factorial design is preferable. The response surface technique is useful when multiple factors influence a reaction or design.

Selecting an acceptable experimental design, identifying the efficient levels/optimum points of several independent parameters, forecasting and testing model equations, and generating contour plots and response surfaces are only some of the goals of the response surface method (RSM) [26]. Cyanide [27], phenol [28], caffeine [29], hexavalent chromium and molybdenum reduction to a less hazardous form [30], and other biological processes optimizations [31-36] have all benefited from RSM's usage to improve biodegradation, biotransformation, and bioremediation.

Using mathematical and statistical programs like Design Expert® and MATLAB®, RSM determines the optimal yield within a predetermined process range. In all that it does, RSM strives to maximize output in light of available means. Visual 2-D and 3-D contour plots of the optimal response show the impact of varying the levels of two components and the possibilities for interactions by adjusting the values of other parameters to achieve the best possible outcome. Visual representations of optimal replies are available [37]. Box Behnken (BB) and Central Composite Design (CCD) are two well-known optimization techniques [38,39]. In this study, the Box-Behnken approach will be selected for the optimization of *E. cloacae* strain UPM2021a growth on acrylamide due to a more compact experimental run needed compared to the CCD.

MATERIALS AND METHODS

All of the chemical reagents utilized in this investigation were employed in the analysis without any further purification. Unless specified otherwise, experiments were conducted in triplicate.

Growth and maintenance of acrylamide-degrading bacterium

The bacterium was isolated from a paddy field in Kepala Batas, which is located in the state of Penang, Malaysia in 2021. The bacterium was grown on Minimal Salts Medium agar that had been supplemented with 1 percent glucose (w/v) as the carbon source and 0.5 g/L (w/v) of acrylamide as the sole nitrogen source. The culture was then shaken at 150 revolutions per minute (rpm) for 72 hours at a temperature of 25 degrees Celsius (Certomat R, USA).

Minimal salt medium (MSM) for growth was supplemented with 0.5 g acrylamide g/L as the sole nitrogen source, glucose 10 g/L as the carbon source, $MgSO_4 \cdot 7H_2O$ 0.5 g/L, KH_2PO_4 6.8 g/L (buffering species and source of phosphorous), $FeSO_4 \cdot H_2O$ 0.005 g/L and 0.1 mL of trace elements [8]. The presence of phosphate in the medium functions as a buffer system, keeping the pH within the range of 5.8 to 7.8 all the time. During the sterilization process, the only source of nitrogen that was used was acrylamide, and the PTFE syringe filters that were utilized had a pore size of 0.45 microns. Samples of one millilitre each were successively diluted in sterile tap water with suitable dilutions (0.5 mL) plated on nutrient agar in order to assess the number of bacteria that were present.

Optimization study using RSM

RSM is a statistical technique used to develop and improve optimization processes to achieve optimal response.[17] In this study, CCD was used as RSM, which is based on three steps such as first, designing and experimental setup; second, response surface modelling through regression; and third, optimization (Du et al., 2010). The relationship and interrelationship between input variables and the experimental response variable were determined by fitting a second-order polynomial equation. The equation is given as:

$$y = \beta_0 + \sum_{i=1}^{k} \beta_i x_i + \sum_{i=1}^{k} \beta_{ii} x_{ii}^2 + \sum_{i=1}^{k-1} \sum_{j>1}^{k} \beta_{ij} x_i x_j + \text{error}$$

where, y is the estimated response variable, β_0 is the regression constant, β_i is the linear regression coefficient, β_{ii} is the quadratic regression coefficient, β_{ij} is the bi-linear regression coefficient.

A three-level, three-factor BBD was employed in this study (**Table 1**). The significant factors from a two-level factorial experiment (published elsewhere) were utilized in this study. The response was bacterial growth measured as log CFU/mL. To reduce fluctuations in observed responses attributable to uncontrollable external influences, the BBD created 17 randomly ordered experimental runs (**Table 2**). To assess the influence of curvature, the experiments collect data from 12 factorial points and 5 centre points located within the experimental zones.

Table 1. Coded and uncoded levels of the independent variables.

Fac-tor	Name	Units	Min-imum	Max-imum	Coded Low	Coded High	Mean	Std. Dev.
A	Acrylamide	g/L	0.3	1.0	-1 ↔ 0.30	+1 ↔ 1.00	0.65	0.2475
B	Incubation	Days	2.0	4.0	-1 ↔ 2.00	+1 ↔ 4.00	3.0	0.7071
C	pH		6.5	7.5	-1 ↔ 6.50	+1 ↔ 7.50	7.0	0.3536

Table 2. Experimental design and results of Box-Behnken for the growth of the bacterium on acrylamide.

Run	Factor 1 A:Acrylamide g/L	Factor 2 B:Incubation Days	Factor 3 C:pH	Response 1 Growth log CFU/mL
1	0.3	3	7.5	3.153
2	0.65	3	7	8.436
3	0.3	3	6.5	3.356
4	0.3	4	7	3.194
5	0.65	2	7.5	4.748
6	1	3	7.5	3.96
7	0.65	3	7	8.5
8	0.65	4	7.5	7.664
9	0.65	2	6.5	7.148
10	0.65	3	7	9.426
11	0.3	2	7	3.756
12	0.65	4	6.5	8.174
13	1	3	6.5	5.823
14	1	4	7	4.824
15	1	2	7	4.724
16	0.65	3	7	9.292
17	0.65	3	7	8.862

In this study, we present the mean results from experiments that were done in triplicates. In order to determine which of these parameters were most important, we ran an analysis using Design Expert 11.0, Stat-Ease, Inc (trial version) and ANOVA.

Statistical Analysis

Values are means ± SD, in triplicate. One-way analysis of variance (with post hoc analysis by Tukey's test) or Student's t-test was used to compare between groups. P-value of < 0.05 was considered was significant.

RESULTS

Box-Behnken experimental design with 3 factors, namely; incubation period (days), acrylamide concentration (g/L) and pH, at 3 different levels (low, medium and high) was employed to investigate the effects on bacterial growth in log CFU/mL as the main response. The produced experimental runs served as the foundation for a series of tests that were carried out. Using the Design-Expert program, mathematical models, including linear, two-factor interaction, and quadratic, were tested for their ability to match the data in order to determine whether or not there was a correlation between the various components and the replies. On the other hand, it is suggested that BB be represented by a quadratic relation, which includes terms that are squared, products of two components, linear terms, and an intercept [40], and this will be used in this study. The design scheme of variables with actual value is illustrated in **Table 3**, along with experimental, predicted values of response and the residuals.

Table 3. The design scheme of variables with experimental, predicted values of response and the residuals.

Run	Factor 1 A: Acrylamide g/L	Factor 2 B: Incubation Days	Factor 3 C: pH	Response. Bacterial growth (log CFU/mL)	Predicted response. log CFU/mL	Residuals
1	0.3	3	7.5	3.15	3.13	0.02
2	0.65	3	7	8.44	8.90	-0.47
3	0.3	3	6.5	3.36	3.55	-0.19
4	0.3	4	7	3.19	3.66	-0.47
5	0.65	2	7.5	4.75	5.40	-0.66
6	1	3	7.5	3.96	3.77	0.19
7	0.65	3	7	8.50	8.90	-0.40
8	0.65	4	7.5	7.66	7.22	0.45
9	0.65	2	6.5	7.15	7.59	-0.45
10	0.65	3	7	9.43	8.90	0.52
11	0.3	2	7	3.76	3.12	0.64
12	0.65	4	6.5	8.17	7.52	0.66
13	1	3	6.5	5.82	5.84	-0.02
14	1	4	7	4.82	5.46	-0.64
15	1	2	7	4.72	4.26	0.47
16	0.65	3	7	9.29	8.90	0.39
17	0.65	3	7	8.86	8.90	-0.04

F-test evaluates the statistical significance of the model, analysis of variance (ANOVA) and P-value of a selected factor is shown in **Table 4**. The results demonstrated that the model is highly significant, which is evident from the F value of 340.53 with a low P-value of <0.0001. The lack of fit p value was not significant which means the model fits well. All factors are significant model terms Computing the correlation coefficient (R2: 0.962, which is closer to unity) and the adjusted correlation coefficient (Adj R2: 0.912), as shown in **Table 4**, verifies the model's reliability. Together, these two coefficients suggest that the model accounts for 91.2 percent of the total variation in response data. With a difference of >0.2 between them, the Predicted R^2 and the Adjusted R^2 were in relatively not reasonable agreement with one another, which may indicate the presenc of an outlier(s). Adeq Precision, which in scientific terms, refers to the ratio of the amount of signal to the amount of noise in an experiment. It is preferable to have a ratio that is bigger than 4. A sufficient signal was obtained with a value of 51.87. Using this paradigm, one may move more easily across the design space. The fact that the Lack of Fit p-value was >0.05 suggests that it is not statistically significant in comparison to the

pure error. Since we want the model to be correct, a lack of fit that is not too large is preferred. The following coded factors (**Table 5**) and equation in terms of actual components can be used to predict growth as the response. The answer for a given level of each factor can be predicted using the equation in terms of actual factors. Here, the levels for each element should be indicated using those very same units. Because the coefficients are scaled to suit the units of each element and the intercept is not at the centre of the design space, this equation should not be used to evaluate the relative impact of each factor.

Table 4. ANOVA analysis of the fitted Box-Behnken design.

Source	Sum of Squares	df	Mean Square	F-value	p-value	
Model	84.62	9	9.40	19.49	0.0004	Signi-ficant
A-Acrylamide	4.31	1	4.31	8.93	0.0203	
B-Incubation	1.51	1	1.51	3.14	0.1198	
C-pH	3.10	1	3.10	6.41	0.0391	
AB	0.1096	1	0.1096	0.2271	0.6482	
AC	0.6889	1	0.6889	1.43	0.2710	
BC	0.8930	1	0.8930	1.85	0.2159	
A^2	61.43	1	61.43	127.31	< 0.0001	
B^2	3.87	1	3.87	8.03	0.0253	
C^2	4.30	1	4.30	8.91	0.0204	
Residual	3.38	7	0.4825			
Lack of Fit	2.57	3	0.8569	4.25	0.0981	not signi-ficant
Pure Error	0.8070	4	0.2018			
Cor Total	88.00	16				

Std. Dev.	0.6946	R^2	0.9616
Mean	6.18	Adjusted R^2	0.9123
C.V. %	11.24	Predicted R^2	0.5183
		Adeq Precision	10.8533

Table 5. The final equation in terms of coded and actual factors.

Coded growth equation	=	Actual Growth equation	=
+8.90		-194.96309	
+0.7340	A	+57.81310	Acrylamide
+0.4350	B	-0.732757	Incubation
-0.6220	C	+54.05603	pH
+0.1655	AB	+0.472857	Acrylamide * Incubation
-0.4150	AC	-2.37143	Acrylamide * pH
+0.4725	BC	+0.945000	Incubation * pH
-3.82	A^2	-31.18041	Acrylamide^2
-0.9591	B^2	-0.959100	Incubation^2
-1.01	C^2	-4.04240	pH^2

Table 6 shows the estimated coefficients of the components that were investigated, together with their respective standard errors, confidence limits, and variance inflation factors (VIF). The variance inflation factor, or VIF, is a statistic that determines how much a lack of orthogonality in the design increases the variance of a certain model coefficient.

When specifically comparing the standard error for a model coefficient in an orthogonal design to the standard error for the same model coefficient in a VIF design, the standard error for the VIF design is greater by a factor equal to the square root of the VIF. As a rule, a VIF of one is desirable since it ensures that the coefficient is orthogonal to the other model components; in other words, the correlation coefficient is zero. On the other hand, VIFs that are greater than ten are cause for worry while VIFs that are greater than one hundred are the reason for concern since they indicate that coefficients were calculated incorrectly owing to multicollinearity, and VIFs that are greater than one thousand are the result of severe collinearity. The value of the VIF for all variables was found to be 1, which suggests that the regression analysis had a significant amount of multicollinearity. The construction of each component's confidence limit is what determines whether or not the regression coefficient of that factor is significant.

Table 6. Coefficients in terms of coded factors.

Factor	Coefficient Estimate	df	Standard Error	95% CI Low	95% CI High	VIF
Intercept	8.90	1	0.3106	8.17	9.64	
A-Acrylamide	0.7340	1	0.2456	0.1533	1.31	1.0000
B-Incubation	0.4350	1	0.2456	-0.1457	1.02	1.0000
C-pH	-0.6220	1	0.2456	-1.20	-0.0413	1.0000
AB	0.1655	1	0.3473	-0.6558	0.9868	1.0000
AC	-0.4150	1	0.3473	-1.24	0.4063	1.0000
BC	0.4725	1	0.3473	-0.3488	1.29	1.0000
A^2	-3.82	1	0.3385	-4.62	-3.02	1.01
B^2	-0.9591	1	0.3385	-1.76	-0.1586	1.01
C^2	-1.01	1	0.3385	-1.81	-0.2101	1.01

According to the OFAT methodology, these were also key contributing parameters in the development of this bacteria on acrylamide (the findings of which were reported elsewhere). This work was carried out using concentrations of acrylamide that were well within the range that has been reported to be tolerated by the majority of bacteria that degrade acrylamide. Acrylamide concentrations that are greater than 1000 mg/L are normally harmful to microorganisms. The propensity of acrylamide to produce alkylation products with the proteins found in microorganisms is the root of its toxicity. A longer incubation period allows for higher growth, and an incubation time ranging from two to five days for optimal development has been recorded in several acrylamide-degrading microorganisms. Therefore, the outcomes of incubation time are something that should be predicted. The majority of microorganisms that degrade acrylamide thrive in circumstances that are close to neutral, which is consistent with the findings of our study and the patterns that have been found in the published literature.

The perturbation plot (**Fig. 1**) of the model exhibits the comparative effect of all the operational parameters at a particular point in the design space. From the plot, it can be observed that factor A (pH) has the steepest curvature. The perturbation plot reveals the presence of two-factor interactions that implies synergistic effects. Moreover, all quadratic effects depicted a significant negative synergistic effect, (A^2), (B^2) and (C^2), at $p < 0.0001$, and the contributions were negative meaning an increase in these factors was detrimental to the response obtained, which is expected as the effect of pH is highly specific within a narrow range whilst higher concentrations of acrylamide are strong growth inhibitory.

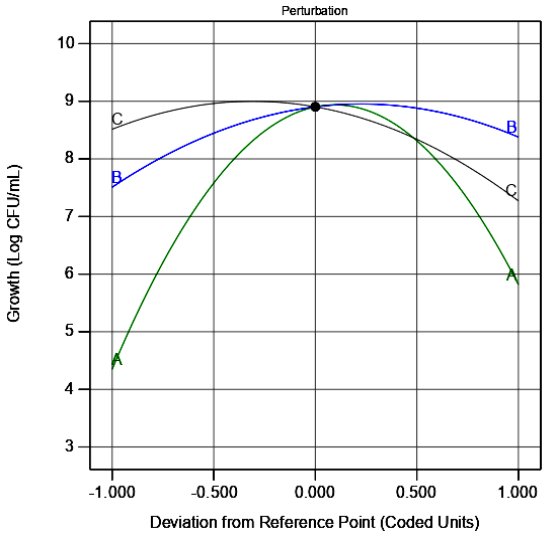

Fig. 1. Perturbation plot of operational parameters obtained for the Box-Behnken design.

In this regard, a half-normal probability plot of the residuals (**Fig. 2**) was constructed and analyzed to ensure the normality assumption. All of the internally studentized residuals values were found to be within 2 and along a straight line, which suggests that there is no requirement for a transformation of the response. This was discovered through research. A good fit may be seen in the graph that compares the actual experimental results to the model's projected values.

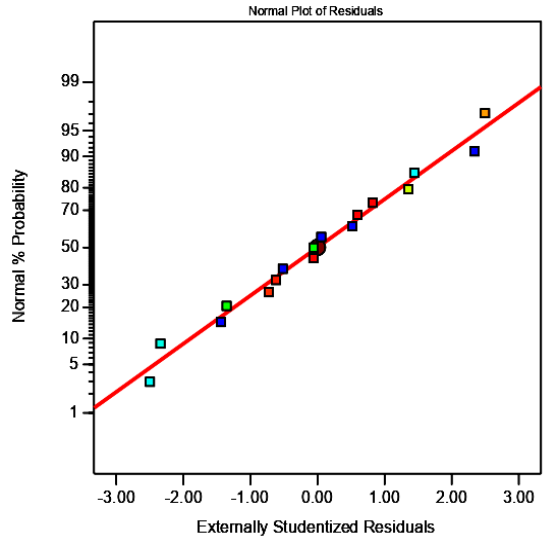

Fig. 2. Normal probability plot of the residuals.

The Box–Cox plot, which can be shown in **Fig. 3**, offers helpful guidance for choosing the appropriate power law transformation based on the value of lambda. Due to the fact that the 95% confidence interval has a value of 1 that corresponds to the value that was designed into the model, it is not advised that any further transformations be made to the observed response in order to fit the model. A good agreement can be seen between the anticipated predicted values and the experimental or observed values when looking at the plot of expected vs real data for the Box-Behnken design (**Fig. 4**). The leverages vs run plot shown in **Fig. 5** reveals that all of the acquired numerical values fall within the usual limits range of 0–1. This indicates the possibility that a design point will have an effect on how the model fits. If there is an issue with the data point, such as an unanticipated error, a high leverage point value of more than one is considered "bad" since the error has a significant impact on the model. According to the plot of leverages vs runs, there are no data that are higher than the average leverage since data that are higher than this would impact at least one model parameter. A measurement of the response outlier that is equivalent to an experimental trial may be obtained from the plot of Cook's distances (**Fig. 6**). Cook's distances are values that cannot be negative, and the higher these values are, the more significant an observation is. For the majority of researchers, the threshold for determining whether or not an observation can be considered important is three times the dataset's mean value of Cook's D. The values of the Cook's distances are determined to be within a value of 1, and this analysis shows the possible presence of outliers especially at runs 5, 11, 12 and 14. The comparison of residuals to run data, as shown in **Fig. 7**, reveals no signs of serial correlation and hints that the data's features are random by nature.

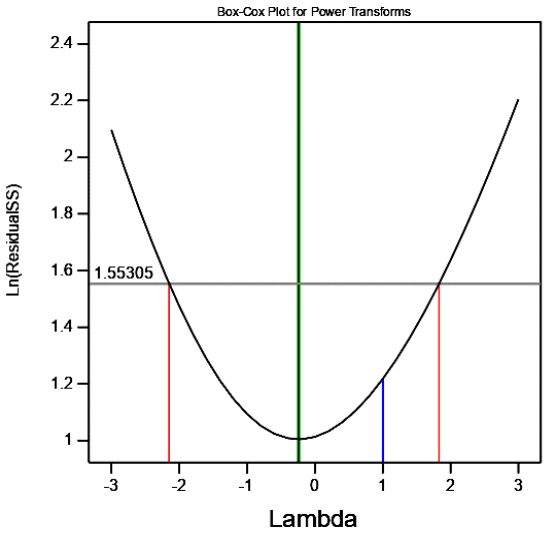

Fig. 3. Diagnostic plot in the form of Box-Cox plot for the Box-Behnken optimization studies.

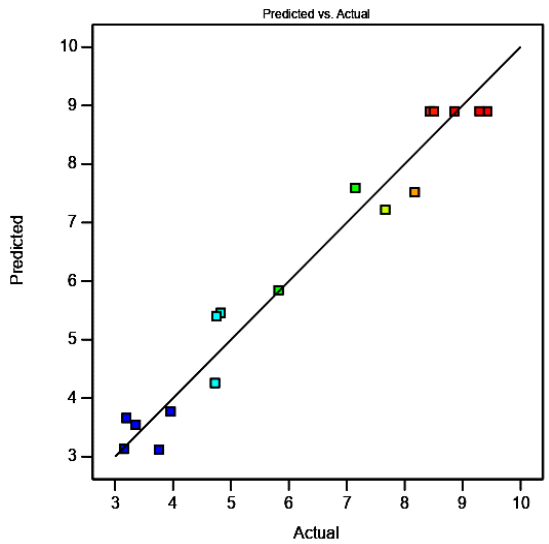

Fig. 4. Diagnostic's plot in the form of the predicted vs real data to the Box-Behnken optimization studies.

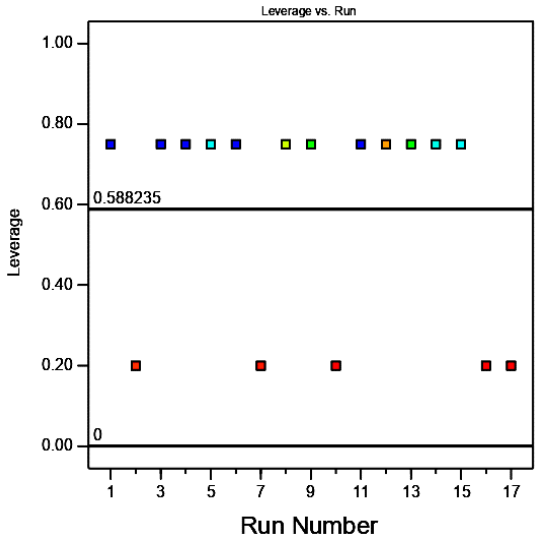

Fig. 5. Diagnostic plot in the form of the leverage vs runs for the Box-Behnken optimization studies.

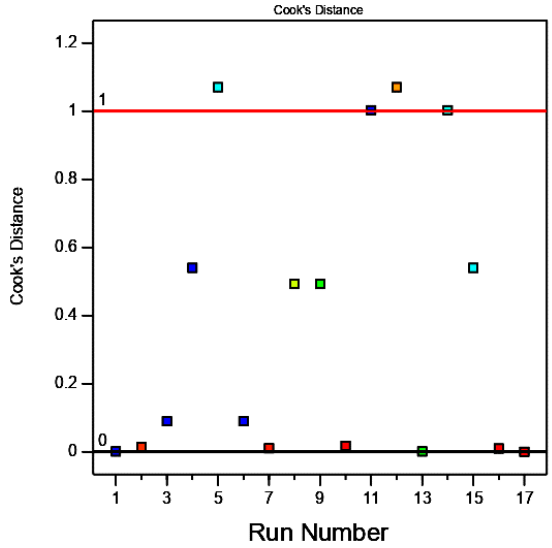

Fig. 6. Diagnostic plot in the form of Cook's distance for the Box-Behnken optimization studies.

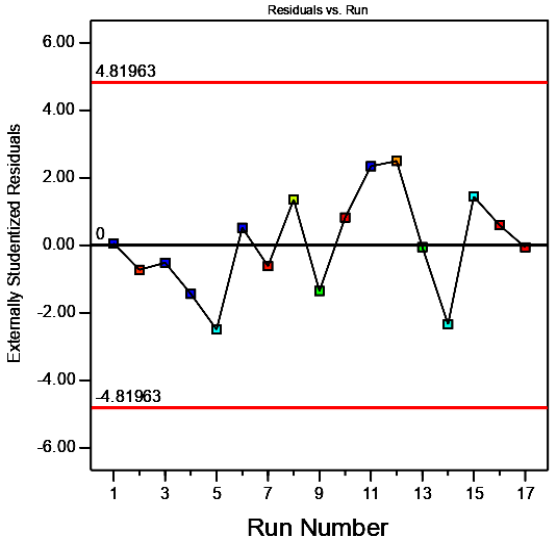

Fig. 7. Diagnostic plot in the form of residuals vs runs for the Box-Behnken optimization studies.

It's not always a problem when influential points are brought up, but it is important to follow up on observations that are marked as extremely influential. A high result on an influence measure could indicate a number of different things, including a mistake in the data input process or an observation that is not typical of the population of interest and so need to be excluded from the analysis. During the process of fitting a model, the inclusion of one or more data points that are sufficiently important might cause coefficient estimations to be thrown off and muddle the model's interpretation. In the past, before conducting a linear regression, the potential of outliers in a dataset would be evaluated using histograms and scatterplots. This was done before running the linear regression.

Both approaches to evaluating data points were subjective, and there was little way to determine how much influence each possible outlier had on the data representing the outcomes. This resulted in the development of a number of quantitative metrics, such as DFFIT and DFBETA. The DFFFITS algorithm assesses how much of an impact each particular example has on the value that was anticipated. It is possible to translate it to the distance according to Cook. DFFITS, in contrast to Cook's distances, can take either a positive or a negative value. When the value is "0," the point in question is located precisely on the regression line. Leverage is what makes this possible.

Mathematically speaking, it is the difference between the expected value with observation and the predicted value without observation. DFFITS is a representation of the externally studentized residual (ti) that has been exaggerated by high leverage points and decreased by low leverage points, as demonstrated by the alternative formula. The plots show the DFBETAS values (**Fig. 8**) and DFFITS values (**Fig. 9**) were within the size-adjusted threshold acceptable range with the exception of several extreme values, which were runs 5, 11, 12 and 14 (DFFITS) (**Table 2**), which can also be seen in the half-normal probability plot above. However, these values barely were above the acceptable range and in overall do not affect the reliability of the model as a whole.

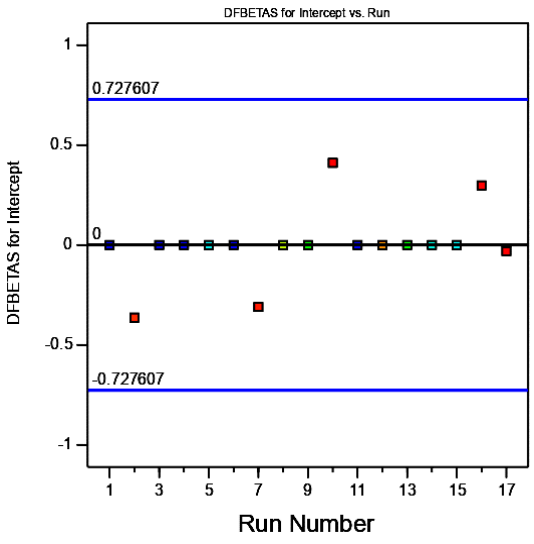

Fig. 8. Diagnostic plot in the form of DFBETAS for intercept vs runs for the Box-Behnken optimization studies.

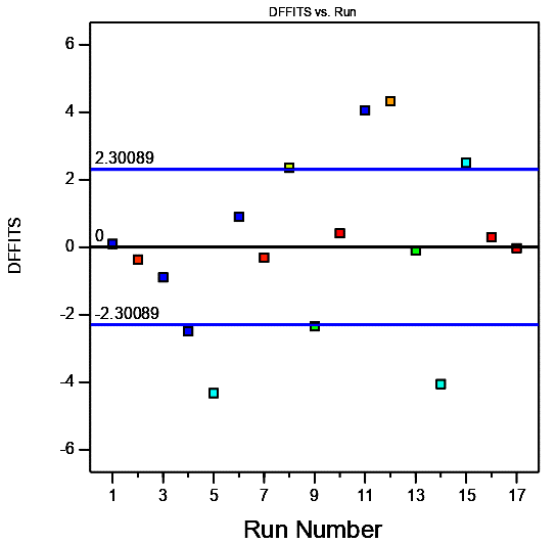

Fig. 9. Diagnostic plot in the form of DFFITS vs runs for the Box-Behnken optimization studies.

The model equation that was provided by the Design Expert program was used to construct the 3D plots, and they were created so that the interaction between the elements could be studied. Charting the answer against any two independent variables on the Z-axis allowed for the creation of three-dimensional displays. In the middle of each of these graphs is a single variable that remains constant, while the other two variables are shown to be changing as the experimental range increases. Each figure illustrates the influence of the reciprocal interaction that occurs between two substantial independent elements, while simultaneously maintaining the status quo for the other two components that were investigated. The shape of the plot is determined by how they influence growth and how they communicate with one another, which are three factors that are independent of one another. When pH was held at the midpoint (7.0), varying the incubation period and acrylamide concentration factors show an elliptical profile indicating a relationship of synergistic interaction (**Fig. 10a**) with the highest response of 8.992 log CFU/mL (95% confidence interval from 8.264 to 9.719) occurring at the predicted acrylamide concentration of 0.69 g/L and incubation period of 3.25 days (desirability of 0.931). Increasing the acrylamide concentration shows an inhibited effect roughly at 0.7 g/L onwards, indicating strong inhibition to bacterial growth, which has been reported in numerous studies [11–20,41–47]. The main negative effect of acrylamide is due to this compound's ability to form adducts with biomolecules in the cell, inactivating their normal function [48–50]. The predicted result was obtained by solving the equation in **Table 5**.

The overall profile indicates a strong inhibition of growth as a response at acrylamide concentrations higher than approximately 0.7 g/L, which is anticipated due to the toxicity of acrylamide at high concentrations to microorganisms in general. The incubation period did not increase by much going from day 2 to day 4 indicating that maximum growth has already been reached after day 2 of incubation. This optimum point occurs in a region that contains predicted points that will not be significantly different from each other ($p>0.05$) as the confidence interval (95%) overlapped. This region occurs between the predicted incubation period of 2.1 days onwards to the studied maximum period of day 4 and acrylamide concentration of between 0.47 and 0.88 g/L (**Fig. 10b**). The elliptical shape of the 3D wired frame and contour plot indicates the mutual interaction between independent factor was significant response surface model [51,52]. Within this bordering region (**Fig. 10c**), the 95% confidence interval of the maximum responses overlapped and was deemed not statistically different ($p>0.05$) [53].

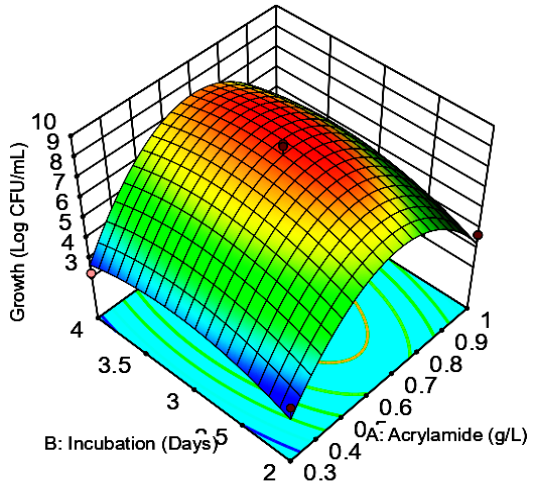

(a)

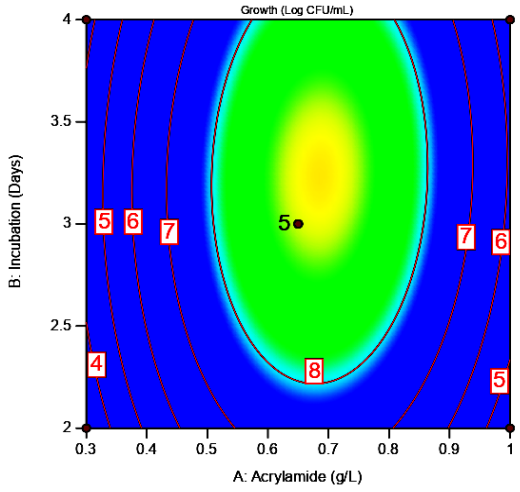

(b)

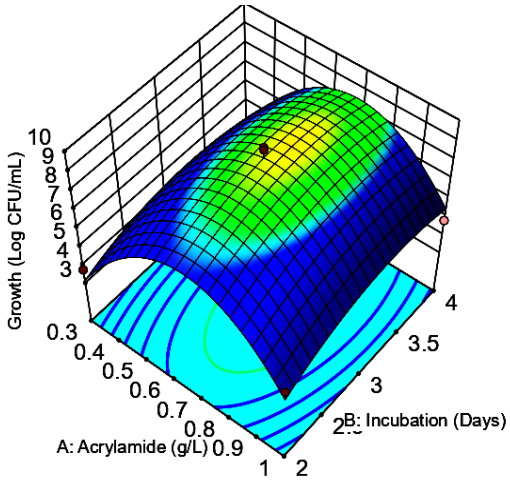

(c)

Fig. 10. The 3D response surface plots of between the factor incubation and acrylamide concentration (a), 95% confidence interval region of optimality visualized as 2D- (b) and 3D- (c) contour plots.

When the incubation period was held at the midpoint (day 3), varying the acrylamide concentration and pH show an elliptical profile indicating a relationship of synergistic interaction (**Fig. 11a**) with the highest response of 9.05 log CFU/mL (95% confidence interval from 8.32 to 9.77) occurring at the predicted points of acrylamide concentration of 0.685 g/L and pH of 6.84 (desirability of 0.940). This optimum point occurs in a region that contains predicted points that will not be significantly different from each other ($p>0.05$) as the confidence interval (95%) overlapped. This region occurs between the predicted of between 6.5 to 7.4 and acrylamide concentrations between onwards to the studied maximum period of day 4 and acrylamide concentration of between 0.47 and 0.90 g/L (**Fig. 11b**). Within this bordering region (**Fig. 11c**), the 95% confidence interval of the maximum responses overlapped and was deemed not statistically different ($p>0.05$) [53].

When acrylamide concentration was held at the midpoint (0.65 g/L), varying the incubation period and acrylamide concentration factors simultaneously show an elliptical profile indicating interaction (**Fig. 12a**). As the pH increases from 6.5 to 7.5 a lowering of growth response was seen indicating unfavourable growth at a higher pH, whilst incubation shows not much difference as the period was increased. The highest response of 9.02 log CFU/mL (95% confidence interval from 8.29 to 9.74) occurred at the predicted incubation period of 3.16 days and pH of 6.89 (desirability of 0.936). This optimum region also occurs between the predicted pH of 6.75 to 7.38 and incubation periods of 2.09 to 4 days (**Fig. 12b**). Within this bordering region (**Fig. 12c**), the 95% confidence interval of the maximum responses overlapped and was deemed not statistically different ($p>0.05$) [53], meaning any points within this region will be similarly optimum statistically ($p>0.05$).

Verification of BB experimental design of RSM for the growth of the bacterium on acrylamide

Predicted optimal conditions were determined using "Numerical Optimisation" toolbox of the Design Expert software. Two optimal conditions were tested. The first was for finding the optimum growth under the range of factors employed whilst the second was to predict the optimum growth at the highest acrylamide concentration tolerable, which was 1.0 g/L. The predicted value of the dependent variable for both sets of design experiments was suggested with different combinations of the parameter value.

Table 7 shows the solutions for the verification of the first predicted model. The model predicted the maximum growth of 9.07 (95% C.I., 8.35 to 9.795) which was verified through experimental results with a growth of 9.94 log CFU/mL (95% C.I., 9.81 to 10.07) with the actual results were near but higher than the predicted value. The predicted combination to give the desired maximum response based on the requirement of **Table 7** was at an acrylamide concentration of 0.691 g/L, incubation period of 3.16 and pH of 6.85. On the other hand, the predicted combination to give the desired maximum response based on the requirement for the conditions where growth at the highest desirable acrylamide concentration is desired as shown in **Table 8** was at an acrylamide concentration of 0.845 g/L, incubation period of 3.18 and pH of 6.81.

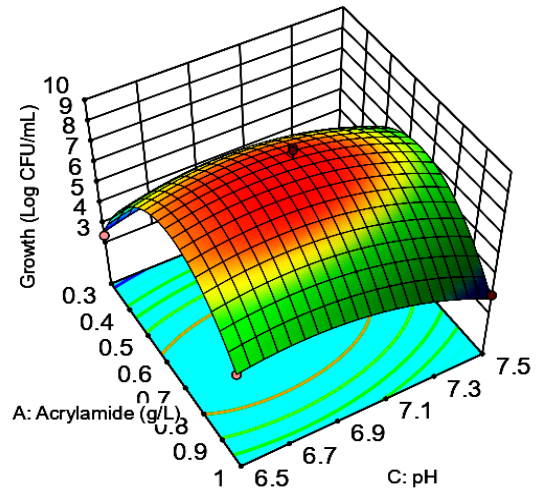

(a)

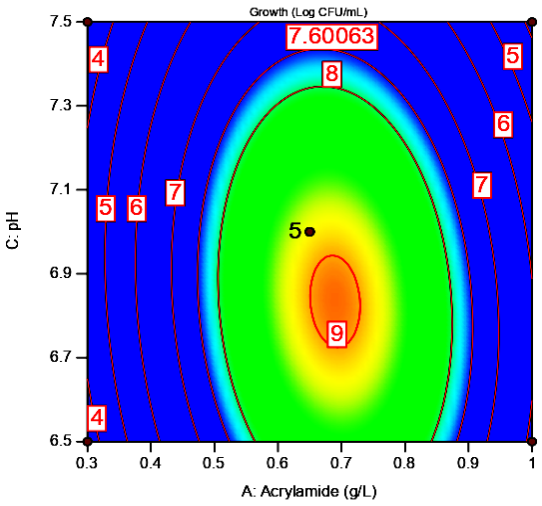

(b)

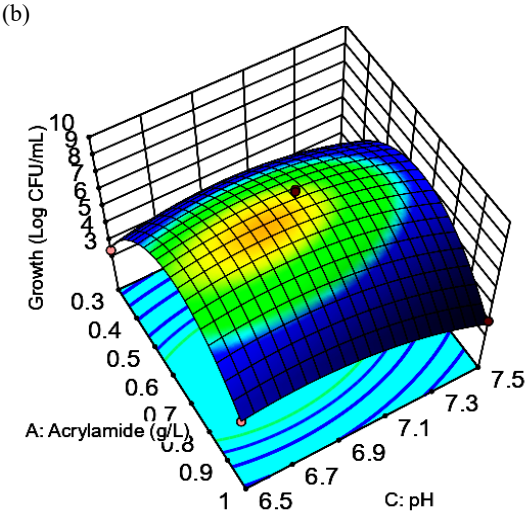

(c)

Fig. 11. The 3D response surface plots between the factor pH and incubation period (a), 95% confidence interval region of optimality visualized as 2D- (b) and 3D- (c) contour plots.

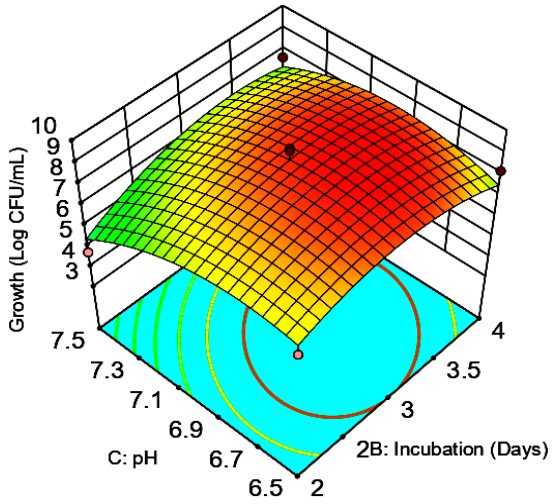

(a)

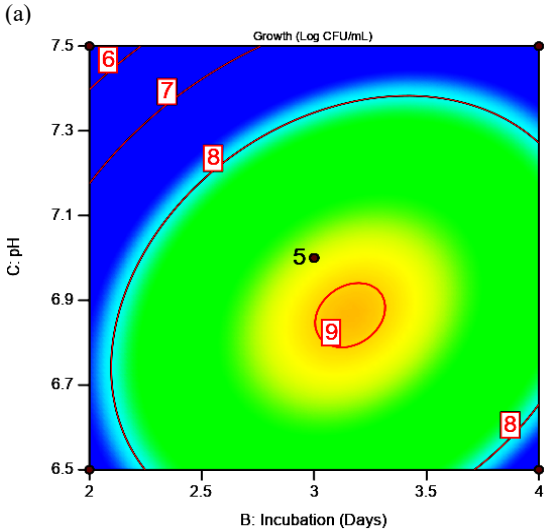

(b)

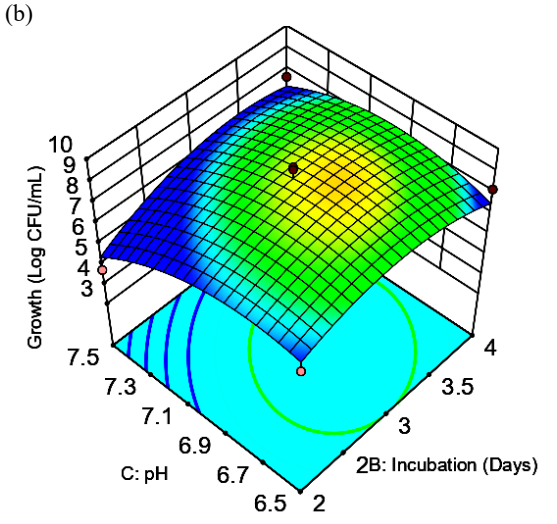

(c)

Fig. 12. The 3D response surface plots of between the factor acrylamide and pH (a), 95% confidence interval region of optimality visualized as 2D- (b) and 3D- (c) contour plots.

The second numerical optimization gave a solution with a predicted maximum growth of 8.338 log CFU/mL (95% C.I. from 7.595 to 9.082), which was verified through experimental results with a growth of 9.56 log CFU/mL (95% C.I. from 9.41 to 9.72) with the actual experimental results were also near but significantly higher than the predicted values. The predicted combination to give the desired maximum response based on the requirement of **Table 8** was at an acrylamide concentration of 0.844 g/L, incubation period of 3.18 and pH of 6.81.

Table 7. Suggested parameter for each variable for maximum growth of the bacterium on acrylamide based on the Box-Behnken design.

Factor	Name	Level	Low Level	High Level	Std. Dev.	Coding
A	Acrylamide	0.6905	0.3000	1.0000	0.0000	Actual
B	Incubation	3.16	2.00	4.00	0.0000	Actual
C	pH	6.85	6.50	7.50	0.0000	Actual

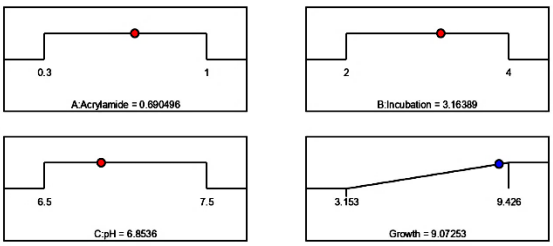

Fig. 13. Desirability ramp for optimization for maximum response with all factors in range. The desirability value was 0.944.

Table 8. Suggested parameter for each variable for maximum growth of the bacterium on maximum acrylamide concentration based on the Box-Behnken design.

Factor	Name	Level	Low Level	High Level	Std. Dev.	Coding
A	Acrylamide	0.8448	0.3000	1.0000	0.0000	Actual
B	Incubation	3.18	2.00	4.00	0.0000	Actual
C	pH	6.81	6.50	7.50	0.0000	Actual

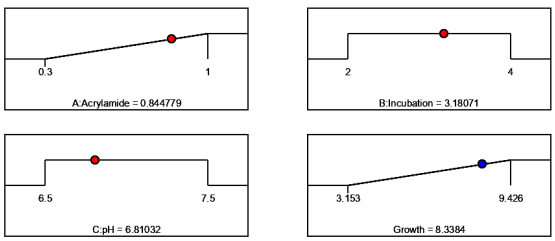

Fig. 14. Desirability ramp for optimization for maximum response with the acrylamide usage factor at maximum whilst other factors are in range. The desirability value was 0.802.

Table 9. Verification results between experiments and predicted response.

RSM target solution	Desira-bility	Predicted mean (95%, C.I.) log CFU/mL	Experimental verification (95%, C.I.)	Statistical significant Difference between predicted and experiment
All factors within range, Maximum growth	0.944	9.07 (8.35 to 9.795)	9.94 (9.81 to 10.07)	Significant Difference ($p<0.05$)
Acrylamide concentration maximum, Maximum growth	0.802	8.338 (7.595 to 9.082)	9.56 (9.41 to 9.72)	Difference is significant ($p<0.05$)

Comparison of optimisation parameters between OFAT and RSM

In comparison, results from OFAT (published elsewhere) and RSM were gathered and compared to each other (**Table 10)**. A statistically better and higher response of about 2 log CFU/mL was achieved through RSM optimisation.

Table 10. Comparison of optimum conditions and results obtained between OFAT and RSM for growth of the bacterium on acrylamide.

	OFAT		RSM	
Factors	Optimum value	Max growth (log CFU/mL)	Optimum value	Max growth (log CFU/mL)
pH	6.5 to 7.5	7.99	6.85	9.94
Incubation period (d)	3		3.16	
Acrylamide (g/L)	0.3 to 1.0		0.691	

When compared to CCD designs, BB designs often feature fewer design points, and as a result, they are easier on the wallet to maintain and operate when resources are few [54]. The Box-Behnken design will never have more than three levels per factor, in contrast to the CCD, which can have as many as five levels per factor [55]. In a Box-Behnken design, the design points are located at combinations of the variables that represent the low, high, and midpoints. For example, if the experiment's operating temperature ranges from 10 to 60 degrees Celsius, the lowest temperature point will be 10 degrees Celsius and the highest temperature point will be 60 degrees Celsius, with 30 degrees Celsius serving as the midway. Box-Behnken does not include a limit breaker, also known as an extreme setting, therefore in contrast to CCD, the minimum temperature will not dip below 10 °C, and the maximum temperature will not rise over 60 °C. When we want our goal scale to stay inside the safe range because of physical or conceptual limits, this feature is quite crucial (e.g., when the temperature starts at zero with no negative range).

Central composite designs are a type of complete fractional factorial design that includes centre points and is complemented by a collection of axial points [55]. As a result, both its upper and lower limits always fall outside of the limit range of the target scale. Box and Behnken (BB) came up with the idea of an incomplete factorial design with three levels as a time-saving replacement for the labour-intensive full factorial design [40]. Polynomials of the second order are required to be utilized in the modelling process in order to effectively capture linear, quadratic, and interaction effects. Box and Behnken came up with this workable concept in order to cut down on the number of tests that were necessary, particularly in the process of fitting quadratic models [40]. +1, 0 and -1 are the three levels of factorial designs that are used for constructing experiment matrices. In order to get the desired level of accuracy in the end product, the core point has been replicated several times. There is not an experimental point in this design at which all of the components have their most extreme values. This capability could come in handy during trials in which unfavourable occurrences might take place as a result of harsh conditions.

In terms of labour efficiency, the Basic Block Design (BB) is only slightly superior to the Central Composite Design (CCD), but it is noticeably superior to the Full Factorial Design (FFD) [52]. The BB has just two key limitations: the number of experimental components must be equal to or more than three, and the BB should not be used to fit equations other than second-order polynomials. Both of these requirements must be met for the BB to be valid [52].

CONCLUSION

The Box-Behnken design was adopted in the optimisation of three factors influencing the growth of the bacterium on acrylamide. These factors include pH, incubation time and acrylamide concentration. The important contributing factors or parameters were analysed using ANOVA, perturbation plots and other diagnostic plots. The diagnostic plots such as half-normal, Cook's distance, residual vs runs, leverage vs runs, Box-Cox, DFFITS, DFBETAS all supported the model with the exception of several extreme values, which were runs 5, 11, 12 and 14 (DFFITS and Cook's distance). Remedies for these outliers in future works include running the experiments in blocks or the outright removal of these outliers. Predicted optimal conditions were determined for finding the optimum growth under the range of factors employed and to predict the optimum, which was 1 g/L. Predicted optimal conditions were determined using "Numerical Optimisation" toolbox of the Design Expert software. Two optimal conditions were tested. The first was for finding the optimum growth under the range of factors employed whilst the second was to predict the optimum growth at the highest acrylamide concentration tolerable, which was 1 g/L. In both verification experiments, the actual results were near the predicted values but were significantly higher than the predicted values. This means that other methods which employ more rus such as CCD or a different optimization approach such as Artificial Neural Network may be employed in the future to close the difference between the model-predicted values and actual experimental values. Despite this, the RSM exercise gave far better growth on acrylamide than OFAT, indicating the utility of RSM over OFAT in the optimization of growth on acrylamide.

REFERENCES

1. Shukor MY, Gusmanizar N, Azmi NA, Hamid M, Ramli J, Shamaan NA, et al. Isolation and characterization of an acrylamide-degrading *Bacillus cereus*. J Enviromental Biol. 2009;30(1):57–64.
2. Spencer P, Schaumburg HH. Nervous system degeneration produced by acrylamide monomer. Environ Health Perspect. 1975 Jun 1;11:129–33.
3. Sega GA, Valdivia Alcota RP, Tancongco CP, Brimer PA. Acrylamide binding to the DNA and protamine of spermiogenic stages in the mouse and its relationship to genetic damage. Mutat Res Mutagen Relat Subj. 1989 Aug 1;216(4):221–30.
4. Tyl RW, Friedman MA. Effects of acrylamide on rodent reproductive performance. Reprod Toxicol. 2003 Jan 1;17(1):1–13.
5. Yang HJ, Lee SH, Jin Y, Choi JH, Han CH, Lee MH. Genotoxicity and toxicological effects of acrylamide on reproductive system in male rats. J Vet Sci. 2005 Jun;6(2):103–9.
6. Backer LC, Dearfield KL, Erexson GL, Campbell JA, Westbrook-Collins B, Allen JW. The effects of acrylamide on mouse germ-line and somatic cell chromosomes. Environ Mol Mutagen. 1989;13(3):218–26.
7. Hagmar L, Törnqvist M, Nordander C, Rosén I, Bruze M, Kautiainen A, et al. Health effects of occupational exposure to acrylamide using hemoglobin adducts as biomarkers of internal dose. Scand J Work Environ Health. 2001;27(4):219–26.
8. Igisu H, Goto I, Kawamura Y, Kato M, Izumi K. Acrylamide encephaloneuropathy due to well water pollution. J Neurol Neurosurg Psychiatry. 1975;38(6):581–4.
9. Rahim MBH, Syed MA, Shukor MY. Isolation and characterization of an acrylamide-degrading yeast *Rhodotorula* sp . strain MBH23 KCTC 11960BP. J Basic Microbiol. 2012;52(5):573–81.
10. Wakaizumi M, Yamamoto H, Fujimoto N, Ozeki K. Acrylamide degradation by filamentous fungi used in food and beverage industries. J Biosci Bioeng. 2009;108(5):391–3.

11. Wampler DA, Ensign SA. Photoheterotrophic metabolism of acrylamide by a newly isolated strain of Rhodopseudomonas palustris. Appl Environ Microbiol. 2005;71(10):5850–7.
12. Buranasilp K, Charoenpanich J. Biodegradation of acrylamide by *Enterobacter aerogenes* isolated from wastewater in Thailand. J Environ Sci. 2011;23(3):396–403.
13. Charoenpanich J, Tani A. Proteome analysis of acrylamide-induced proteins in a novel acrylamide-degrader *Enterobacter aerogenes* by 2D electrophoresis and MALDI-TOF-MS. Chiang Mai Univ J Nat Sci. 2014;13(1):11–22.
14. Gusmanizar N, Shukor Y, Ramli J, Syed MA. Isolation and characterization of an acrylamide-degrading *Burkholderia* sp. strain DR.Y27. J Ris Kim. 2015 Feb 11;2(1):34.
15. Yu F, Fu R, Xie Y, Chen W. Isolation and characterization of polyacrylamide-degrading bacteria from dewatered sludge. Int J Environ Res Public Health. 2015;12(4):4214–30.
16. Bedade DK, Singhal RS. Biodegradation of acrylamide by a novel isolate, *Cupriavidus oxalaticus* ICTDB921: Identification and characterization of the acrylamidase produced. Bioresour Technol. 2018 Aug 1;261:122–32.
17. Aisami A, Gusmanizar N. Characterization of an acrylamide-degrading bacterium isolated from hydrocarbon sludge. Bioremediation Sci Technol Res. 2019 Dec 28;7(2):15–9.
18. Othman AR, Rahim MBHA. Modelling the Growth Inhibition Kinetics of *Rhodotorula* sp. strain MBH23 (KCTC 11960BP) on Acrylamide. Bioremediation Sci Technol Res. 2019 Dec 28;7(2):20–5.
19. Rusnam, Gusmanizar N. An Acrylamide-degrading Bacterial Consortium Isolated from Volcanic Soil. J Biochem Microbiol Biotechnol. 2021 Dec 31;9(2):19–24.
20. Rusnam, Gusmanizar N. Characterization of An Acrylamide-degrading Bacterium Isolated from Volcanic Soil. J Environ Bioremediation Toxicol. 2022 Aug 5;5(1):32–7.
21. Madondo NI, Chetty M. Anaerobic co-digestion of sewage sludge and bio-based glycerol: Optimisation of process variables using one-factor-at-a-time (OFAT) and Box-Behnken Design (BBD) techniques. South Afr J Chem Eng. 2022 Apr 1;40:87–99.
22. Kumar P, Sudesh, Kumar A, Suneja P. Studies on the physicochemical parameter's optimization for indole-3-acetic acid production by Pantoea agglomerans CPHN2 using one factor at a time (OFAT) and response surface methodology (RSM). Environ Sustain [Internet]. 2022 Dec 13 [cited 2023 Jan 2]; Available from: https://doi.org/10.1007/s42398-022-00254-5
23. Zhang D, Zhang K, Hu X, He Q, Yan J, Xue Y. Cadmium removal by MgCl2 modified biochar derived from crayfish shell waste: Batch adsorption, response surface analysis and fixed bed filtration. J Hazard Mater. 2021 Apr 15;408:124860.
24. Yap LS, Lee WL, Ting ASY. Optimization of L-asparaginase production from endophytic Fusarium proliferatum using OFAT and RSM and its cytotoxic evaluation. J Microbiol Methods. 2021 Dec 1;191:106358.
25. Sam SP, Adnan R, Ng SL. Statistical optimization of immobilization of activated sludge in PVA/alginate cryogel beads using response surface methodology for p-nitrophenol biodegradation. J Water Process Eng. 2021 Feb 1;39:101725.
26. Khuri IA, Mukhopadhyay S. Response surface methodology. Adv Rev WIREs Comput Stat John Wiley Sons Inc. 2010;2:128–49.
27. Karamba KI, Ahmad SA, Zulkharnain A, Syed MA, Khalil KA, Shamaan NA, et al. Optimisation of biodegradation conditions for cyanide removal by *Serratia marcescens* strain AQ07 using one-factor-at-a-time technique and response surface methodology. Rendiconti Lincei. 2016 Sep;27(3):533–45.
28. Annadurai G, Ling LY, Lee J fwu. Statistical optimization of medium components and growth conditions by response surface methodology to enhance phenol degradation by *Pseudomonas putida*. J Hazard Mater. 2008;151:171–8.
29. Ibrahim S, Shukor MY, Khalil KA, Halmi MIE, Syed MA, Ahmad SA. Application of response surface methodology for optimising caffeine-degrading parameters by *Leifsonia* sp. strain SIU. J Environ Biol. 2015 Sep;36(5):1215–21.
30. Ahmad WA, Zakaria ZA, Zakaria Z, Surif S. Hexavalent Chromium Reduction at Different Growth Phases of Acinetobacter haemolyticus. 2009;26(7):1275–8.
31. Mishra S, Maiti A. Process optimization for effective bio-decolourization of Reactive Orange 16 using Chemometric methods. J Environ Sci Health Part A. 2018 Nov 6;
32. Wang GL, Li XF, Zhang H, Xiong MH, Li F. Optimization of CTN-4 to chlorothalonil-degrading conditions and a kinetics model. Zhongguo Huanjing KexueChina Environ Sci. 2013;33(11):1999–2005.
33. Mao J, Lee SY, Won SW, Yun YS. Surface modified bacterial biosorbent with poly(allylamine hydrochloride): Development using response surface methodology and use for recovery of hexachloroplatinate(IV) from aqueous solution. Water Res. 2010;44(20):5919–28.
34. Zhang J, Lin G, Yin X, Zeng J, Wen S, Lan Y. Application of artificial neural network (ANN) and response surface methodology (RSM) for modeling and optimization of the contact angle of rice leaf surfaces. Acta Physiol Plant. 2020 Mar 29;42(4):51.
35. Amdoun R, Khelifi L, Khelifi-Slaoui M, Amroune S, Asch M, Assaf-Ducrocq C, et al. The Desirability Optimization Methodology; a Tool to Predict Two Antagonist Responses in Biotechnological Systems: Case of Biomass Growth and Hyoscyamine Content in Elicited Datura starmonium Hairy Roots. Iran J Biotechnol [Internet]. 2018 Apr 18 [cited 2020 Mar 29];16(1). Available from: https://www.ncbi.nlm.nih.gov/pmc/articles/PMC6217265/
36. Sridevi V. Biosorption of methylene blue by spent biomass of Aspergillus terreus using response surface methodology. Int J Pharma Bio Sci. 2013;4(4):P317–25.
37. Anderson MJ, Whitcomb PJ. RSM simplified: optimizing processes using response surface methods for design of experiments. 2nd ed. Boca Raton, FL, USA.: Productivity Press; 2016.
38. Halmi MIE bin, Abdullah SRS, Wasoh H, Johari WLW, Ali MS bin M, Shaharuddin NA, et al. Optimization and maximization of hexavalent molybdenum reduction to Mo-blue by *Serratia* sp. strain MIE2 using response surface methodology. Rendiconti Lincei. 2016 Dec 1;27(4):697–709.